Application of the NUFFT for Reconstruction Problems in Diffraction Tomography

Michael M. Bronstein, Alexander M. Bronstein, Michael Zibulevsky
Department of Electrical Engineering, Technion – Israel Institute of Technology.

Haim Azhari
Department of Biomedical Engineering, Technion – Israel Institute of Technology.

1. Introduction

Ultrasound tomography with diffracting sources is an important type of acoustic imaging. Since the used wave-lengths are comparable to the object feature dimensions, the straight ray tomography theory is no more applicable. Particularly, the Fourier Slice Theorem should be replaced by the Fourier Diffraction Theorem [1], [2].

Reconstruction methods used beforehand addressed the problem as straightforward approximation of the inverse non-uniform Fourier transform (NUFT) and involved frequency interpolation [1], [8], which is liable to introduce significant inaccuracies. More accurate and computationally efficient methods [3], [4] were proposed for forward and inverse 1D NUFT.

Recently, fast and accurate approximation of the forward non-uniform Fourier transform was introduced by Fessler and Sutton [5]. Inverse NUFFT can be achieved iteratively in this framework. We adopt this approach for iterative reconstruction in diffraction tomography, combining it with total variation regularization [6], [7] in order to suppress noise while preserving the sharpness of edges. Simulation studies with the Shepp-Logan phantom show that the proposed algorithm significantly outperforms the frequency interpolation methods.

2. Principles of diffraction tomography

Diffraction tomography allows reconstructing the refractive index $\gamma(\boldsymbol{x})$ of a scattering object by processing the data obtained in scattering experiments [1]. In the classical configuration, the object is illuminated with a plane acoustic wave with wave number $K = 2\pi/\lambda$ and temporal frequency $\omega = 2\pi c/\lambda$, propagating in direction θ:

$$\psi_\theta(\boldsymbol{x},t) = \exp(-\bullet\omega t)\exp(\bullet K\boldsymbol{x}\cdot\theta) \triangleq \exp(-\bullet\omega t)u_\theta(\boldsymbol{x}) \qquad (1)$$

The resulting field $u(\boldsymbol{x})$ satisfies the reduced wave equation

$$\Delta u(\boldsymbol{x}) + K^2\left(1+f(\boldsymbol{x})\right)u(\boldsymbol{x}) = 0 \;\; ; \;\; f(\boldsymbol{x}) = \gamma^2(\boldsymbol{x}) - 1 \qquad (2)$$

where Δ denotes the Laplacian operator. $u(\boldsymbol{x})$ can be written as a superposition of the *incident field* $u_\theta(\boldsymbol{x})$, computed under the assumption of a homogeneous medium, and the *scattered field* $u_s(\boldsymbol{x})$, attributed solely to the inhomogeneities [1]. The scattered field is measured along a line of detectors. Equation (2) can be rewritten in an integral form, known as the *Lippmann-Schwinger integral equation*:

$$u_s(\boldsymbol{x}) = -K^2\int_\Omega G(\boldsymbol{x}-\boldsymbol{y})f(\boldsymbol{y})u(\boldsymbol{y})d\boldsymbol{y} \qquad (3)$$

where $G(\boldsymbol{x})$ is the appropriate Green function.

Reconstruction is possible by linearization of (3). The *Born approximation* is obtained by assuming weak scattering ($u(\boldsymbol{x}) \approx u_\theta(\boldsymbol{x})$). Under the assumption of the Born approximation, a possible alternative is solving the inverse problem in the frequency domain.

3. The Fourier diffraction theorem

Given a projection $P_\theta(r)$ of the forward scattered field $u_s(\boldsymbol{x})$ obtained by illuminating an object $f(\boldsymbol{x})$ with a plane wave, the following equation holds:

$$\bullet\{P_\theta(r)\}(\omega) = \bullet_{2D}\{f(\boldsymbol{x})\}(K(\omega)) \qquad (4)$$

where

$$K_x(\omega) = \omega\cos\theta - \left(\sqrt{K_0^2-\omega^2}-K_0\right)\sin\theta \;\; ; \;\; K_y(\omega) = \omega\sin\theta + \left(\sqrt{K_0^2-\omega^2}-K_0\right)\cos\theta \;\; ; \;\; K_0 = \frac{2\pi}{\lambda} \qquad (5)$$

and $\bullet\bullet$ and $\bullet_{2D}$ denote the one- and the two-dimensional Fourier transforms, respectively. In other words, the Fourier

Authorized licensed use limited to: Institute of Science and Technology Austria (IST). Downloaded on September 23,2026 at 11:25:47 UTC from IEEE Xplore. Restrictions apply.

transform of the projection gives the values of the 2D Fourier transform of the object along a semi-circular arc in the spatial frequency domain, as depicted in Figure 1 [1].

Since wave phenomena obey the superposition principle, illuminating the object with a wave consisting of a set of frequencies (referred to as *broadband illumination*), rather than a monochromatic wave, will produce samples along a set of semi-circular arcs with different radii. Hence, a single projection contains more information about the object than a single projection in straight ray tomography, and sufficient image quality can be achieved with fewer projections.

Two main reconstruction strategies in diffraction tomography are interpolation in frequency domain (analogous to the direct Fourier inversion in straight ray tomography) and interpolation in space domain (analogous to the filtered backprojection), usually termed as *backpropagation* [1], [2]. A common way for image reconstruction in the frequency domain is the gridding algorithm [1], [8]. The non-uniform data is interpolated to a uniform Cartesian grid using, for example, polynomial interpolation. Afterwards, the inverse Fourier transform is efficiently computed using FFT. However, this approach is liable to introduce inaccuracies and is sensitive to the configuration of the sample points. In the next part, we introduce an iterative reconstruction method, which allows reconstruct the image from non-uniform samples in frequency domain without using gridding.

4. Non-Uniform Fourier Transform

The heart of iterative image reconstruction from non-uniform frequency samples is the forward non-uniform fast Fourier transform. To define the NUFFT problem, we first consider a one-dimensional case. Let $\xi = (\xi_1,...,\xi_K) : \xi_k \in [-\pi,\pi]$ be a vector of non-uniformly distributed frequencies and $f = (f_{-N/2},...,f_{N/2-1}) : f_n \in \mathbb{C}$ be a vector of samples of a signal. The non-uniform Fourier transform is the following trigonometric polynomial

$$F_k = \sum_{n=-N/2}^{N/2-1} f_n \exp(-in\xi_k) \tag{6}$$

In matrix notation, $F = \Psi f$, where $\Psi \in \mathbb{C}^{K\times N}$ $(K \geq N)$ is a full column rank matrix containing K discrete exponent functions in its rows: $\Psi = (\psi_1;...;\psi_K)$; $\psi_k(n) = \exp(-in\xi_k)$. Fast approximation $\cdot\cdot$ of the NUFT operator can be achieved by projecting the signal f on some oversampled uniform Fourier basis $\Phi \in \mathbb{C}^{qK\times N}$ using standard FFT, with consequent efficient interpolation:

$$F \approx \cdot f = \mathrm{U}_p \Phi f \tag{7}$$

where U_p denotes the interpolation operator, which makes use of p neighboring uniform samples for approximation of each non-uniform sample and q is the oversampling factor. The overall complexity of such an algorithm is $O(qN\log qN + pK)$.

Selecting the interpolation coefficients U_p is a problem *per se*, and there are many ways of doing it. Recently, Fessler and Sutton [5] proposed obtaining such interpolation coefficients that minimize the maximum approximation error at a given point of the non-uniform grid over all signals with unit l_2-norm. This approach can be formulated as a min-max problem:

$$\min_{u_k} \max_{\|f\|_2 \leq 1} \left| u_k \Phi_p^k f - \psi_k f \right|^2 \tag{8}$$

where u_k is the non-zero part of the k-th row of the interpolation matrix U_p, and Φ_p^k is a part of the overcomplete DFT basis Φ, containing p nearest neighbors of the non-uniform basis element ψ_k. The problem has an analytic solution:

$$u_k = \psi_k \Phi_p^{k\,\mathrm{H}} \left(\Phi_p^k \Phi_p^{k\,\mathrm{H}} \right)^{-1} \tag{9}$$

corresponding to the coefficients of the best approximation of ψ_k in Φ_p^k (superscript H denotes Hermitian transpose). In practice, the interpolation coefficients can be pre-computed.

5. Iterative solution of the inverse problem

A. Formulation of the optimization problem

Straightforward solution of the inverse problem of (7) is a computationally extensive operation. It is given by the Moore-Penrose pseudoinverse:

$$f = \Psi^+ F = \left(\Psi^{\mathrm{H}} \Psi \right)^{-1} \Psi^{\mathrm{H}} F \tag{10}$$

Authorized licensed use limited to: Institute of Science and Technology Austria (IST). Downloaded on September 23,2026 at 11:25:47 UTC from IEEE Xplore. Restrictions apply.

However, such a solution is practically impossible when N is large. Alternatively, equation (10) can be reformulated as an optimization problem:

$$\min_f \left\| \cdot f - F \right\|_2^2 \tag{11}$$

It is possible to add penalty on some kind of signal irregularity to the object function:

$$\min_f \left\| \cdot f - F \right\|_2^2 + \mu\varphi(f) \tag{12}$$

where μ is a parameter controlling the influence of the penalty. Such a penalty approach is usually referred to as Tikhonov regularization. This problem can be solved iteratively using various large-scale optimization techniques, which require efficient computation of the objective function and its gradient [9].

B. Total variation regularization

Empirical observations show that the majority of images that occur in nature, and particularly in medical imaging applications, belong to the class of functions of bounded total variation (defined as the integral of the gradient l_2-norm) [10]. The penalty term for total variation can be used in problem (12). For discrete image, the smoothed total variation is given by

$$TV(f) = \sum_{i,j} \sqrt{(f_x)_{ij}^2 + (f_y)_{ij}^2} \tag{13}$$

where f_x, f_y are the discrete directional derivatives of the image, and η is a small positive smoothing parameter. Total variation regularization removes small oscillations resulting from noise and Gibbs phenomena, without significantly affecting the edges.

6. Results

Reconstruction was simulated on the analytic Shepp-Logan phantom, using the conjugate gradients optimization algorithm.

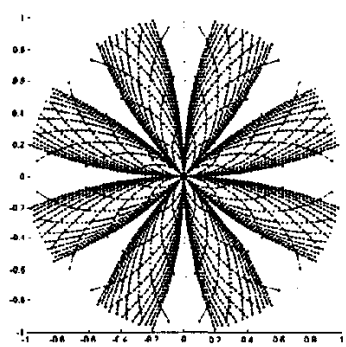


Figure 1: Frequency domain sampling corresponding to 8 broadband projections (normalized spatial frequency).

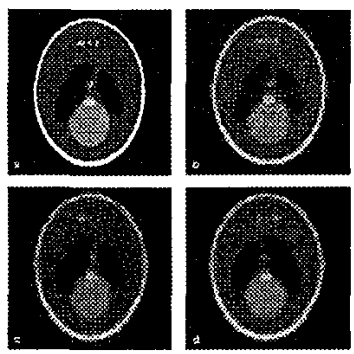


Figure 2: a. original band-unlimited phantom, b. reconstruction by gridding, c. iterative least-squares reconstruction, d. iterative reconstruction with total variation penalty (μ = 100).

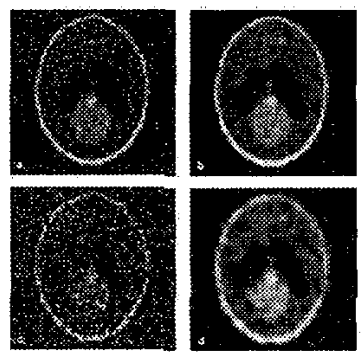


Figure 3: Iterative reconstruction in presence of noise (a, b: SNR = 20dB, c, d: SNR = 10dB) with total variation penalty μ = 100 (b, d) and without penalty (a, c).

[1] A. C. Kak and M. Slaney, *Principles of Computerized Tomographic Imaging*, Society of Industrial and Applied Mathematics, 2001.
[2] A. J. Devaney, A filtered backpropagation algorithm for diffraction images, *Ultrasonic imaging*, Vol. 4, pp. 336-350, 1982
[3] G. Beylkin, "On the fast Fourier transform of function with singularities", *Applied and Computational Harmonic Analysis* 2, pp. 363-381, 1995.
[4] A. Dutt and V. Rokhlin, "Fast approximate Fourier transforms for nonequispaced data", *SIAM J. Sci. Comput.*, Vol. 14, No. 6, pp. 1368-1393, November 1993.
[5] J. Fessler and B. P. Sutton, "Non-uniform fast Fourier transforms using min-max interpolation", submitted to *IEEE Trans. Signal Processing*, 2001.
[6] L. I. Rudin, S. Osher and E. Fatemi, Nonlinear total variation based noise removal algorithms, *Physica D*, vol. 60, pp. 259-268, 1992
[7] P. Blomgren, T. F. Chan, P. Mulet and C. K. Wong, Total variation image restoration: numerical methods and extensions, Proc. ICIP 97.
[8] F.T.A.W. Wajer, R. Lethmate, J.A.C. van Osch, D. Graveron-Demilly, M. Fuderer and D. van Ormondt, "Interpolation from arbitrary to Cartesian sample positions: gridding", Proceedings *ProRISC/IEEE Workshop*, 2000.
[9] D. P. Bertsekas, *Nonlinear Programming*, 2nd ed., Athena Scientific, 1999.
[10] S. Mallat, *A Wavelet Tour of Signal Processing*, 2nd ed., Academic Press, 1999.
[11] M. Bronstein, A. Bronstein and M. Zibulevsky, "Iterative reconstruction in diffraction tomography using NUFFT", *IEEE Transactions on Medical Imaging*, in press, 2002. Available: http://visl.technion.ac.il/bron/works

Authorized licensed use limited to: Institute of Science and Technology Austria (IST). Downloaded on September 23,2026 at 11:25:47 UTC from IEEE Xplore. Restrictions apply.